DOI: 10.1002/chem.200700800

A Hydrophilic Cyclodextrin Duplex Forming Supramolecular Assemblies by Physical Cross-Linking of a Biopolymer

Olivia Bistri,[a] Karim Mazeau,[b] Rachel Auzély-Velty,*[b] and Matthieu Sollogoub*[a]

Abstract: New β-cyclodextrin (β-CD) dimeric species have been synthesised in which the two CD moieties are connected by one or two hydrophilic oligo(ethylene oxide) spacers. Their complexation with sodium adamantylacetate (free adamantane) and adamantane-grafted chitosan (AD-chitosan) was then studied by different complementary techniques and compared with their hydrophobic counterparts that contain an octamethylene spacer. Isothermal titration calorimetry experiments have demonstrated that the use of hydrophilic spacers between the two CDs instead of aliphatic chains makes almost all of the CD cavities available for the inclusion of free adamantane. Investigation of the interaction of the CDs with AD-chitosan by viscosity measurements strongly suggests that the molecular conformation of the CD dimeric species plays a crucial role in their cross-linking with the biopolymer. The derivative doubly linked with hydrophilic arms, also called a duplex, has been shown to be a more efficient cross-linking agent than its singly bridged counterpart, referred to as a dimer. Hence, only 0.5 molar equivalents of the hydrophilic duplex with respect to adamantane was required to obtain the maximum viscosity, whereas in the case of the duplex with aliphatic spacers, the maximum viscosity was achieved with a [duplex]/[AD] ratio of about 1.7 (corresponding to a [CD]/[AD] ratio of 2.5), but with a higher value. To clarify the relationships between the molecular architecture and complexation properties, computational studies were also performed that clearly confirmed the importance of double bridging.

Keywords: calorimetry · cyclodextrins · molecular modeling · physical cross-linking · viscometry

Introduction

Bridged cyclodextrin (CD) dimers have been widely studied because favourable cooperative binding effects, owing to multivalency, may occur that lead to significantly higher binding constants than those of the monomeric species.[1–5] Such derivatives are generally obtained by connecting the two CDs through their primary side, although bridging them through the secondary side seems to be more logical because guest binding usually takes place at the wider secondary side of CDs. Ease of synthesis is one of the main reasons for the relatively large number of CD dimers linked through their primary side. Nevertheless, with some of them, and with appropriate ditopic guests, very high association constants of up to $10^{10}\,\mathrm{M}^{-1}$ could be obtained.[1] The principal structural feature of these dimers is the double linkage that is supposed to provide rigidity in the host molecule, thus limiting conformations that are not involved in guest binding. This distinctive feature, compared with singly linked dimers, led the authors to coin the name duplex CDs for this family of dimers.[6] Herein, we will therefore refer to doubly bridged CD dimers as duplexes and to singly bridged derivatives as dimers. The main drawback of duplexes is the inherent difficulties encountered in their synthesis.[6] Recently, we have developed an efficient method for the preparation of $6^A,6^D$-diols from fully benzylated α- and β-CDs.[7] As illustrated in Figure 1, with β-CD as an example, a truncated cone is commonly used to represent the CD torus, and therefore, the $6^A,6^D$-diol is conveniently depicted as shown on the right side of the figure.

[a] Dr. O. Bistri, Dr. M. Sollogoub
Université Pierre et Marie Curie-Paris 6
Institut de Chimie Moléculaire (FR 2769), ENS
Département de Chimie, UMR CNRS 8642, 75005 Paris (France)
Fax: (+33) 144-323-397
E-mail: matthieu.sollogoub@upmc.fr

[b] Dr. K. Mazeau, Prof. R. Auzély-Velty
Centre de Recherches sur les Macromolécules Végétales (CERMAV-CNRS), BP53
38041 Grenoble Cedex 9 (France)
(Affiliated to Université Joseph Fourier and a member of the Institut de Chimie Moléculaire de Grenoble (France)).
Fax: (+33) 476-547-203
E-mail: Rachel.Auzely@cermav.cnrs.fr

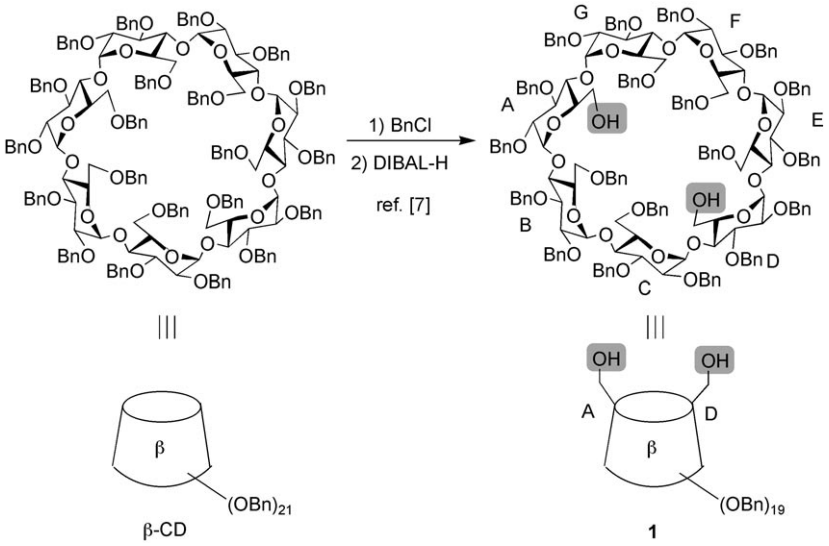

Figure 1. Representations of the CDs and the structure of $6^A,6^D$-diol **1**.

These diols can be efficiently converted into homo-dimers that are singly and doubly linked with octamethylene spacers, which leads to the formation of dimer **2** and duplex **3**, respectively.[8] An investigation of the complexation properties of the β-CD dimeric species towards adamantane-grafted chitosan (AD-chitosan) by viscosity measurements showed that **3** could efficiently increase the viscosity of aqueous solutions of the modified polysaccharide, whereas its singly connected counterpart, **2**, did not have this effect.[9] These different abilities to physically cross-link modified chitosan chains were related to different molecular flexibilities and inclusion properties of the CD dimeric species. Indeed, calorimetric titration measurements demonstrated that the binding of sodium adamantylacetate (ADAc) by **3** is 11 times stronger than that by **2** and three times stronger than that by natural β-CD. This strong binding was attributed to a strengthening of hydrophobic interactions owing to the presence of the two C_8 hydrophobic chains that connect the CD cavities. On the other hand, only some of the cavities (about one half) in both **2** and **3** were shown to be available for binding; this could be explained by the inclusion of the spacers in the CD cavities to favour the formation of aggregates, as shown by NMR spectroscopy. The formation of aggregates is also promoted by the amphiphilic nature of **2** and **3**. These results led us to envisage the preparation of new CD dimeric species **4** and **5**, in which the two CD moieties are connected by one or two hydrophilic oligo(ethylene oxide) spacers to limit the assumed formation of aggregates. Indeed, our aim was to obtain CD dimeric species able to efficiently cross-link hydrophobically modified biopolymers leading to reversible networks.

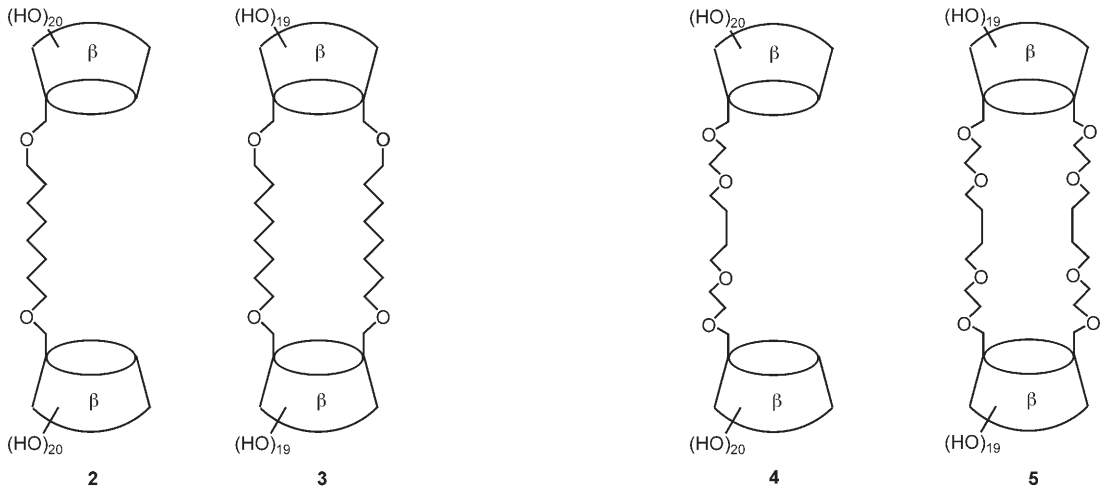

In this paper, we report the synthesis of these new CD derivatives **4** and **5** and compare their complexation properties with ADAc and AD-chitosan with those of the dimeric species that contain aliphatic spacers.

Results and Discussion

Synthesis: Our strategy towards the synthesis of **4** and **5** was based on the metathesis reaction.[8,10] Key intermediate monomeric CD **6** was easily synthesised from β-CD through the now classical benzylation–debenzylation sequence[7] followed by the selective mono-etherification of **1** with **7**[11] in

a yield of 67% (Scheme 1). As already alluded to, compound **6** is a mixture of two regioisomers, $6^A,6^D$-β-CD and $6^A,6^E$-β-CD, and so are the following dimeric species.

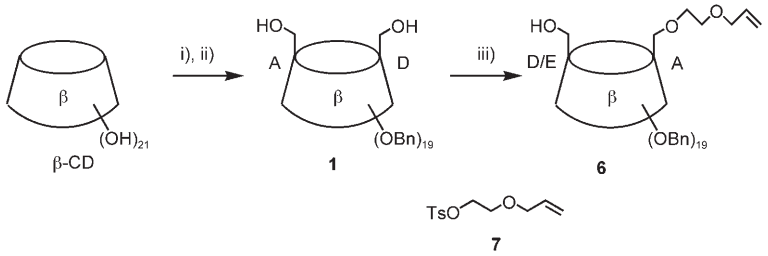

Scheme 1. Synthesis of monomer **6**. Reagents and conditions: i) BnCl, NaH, DMSO, RT, 12 h, 95%; ii) iBu$_2$AlH, toluene, 1 h, 50°C, 84%; iii) **7**, KH, nBu$_4$NI, THF, RT, 18 h, 67%.

Self-metathesis of **6** in the presence of a first-generation Grubbs catalyst gave unsaturated dimer **8** in a yield of 62%. Saturation of the double bond had to be performed by using tosyl hydrazide instead of the usual hydrogenation conditions, which consistently resulted in hydrogenolysis of the allyl to give **9** in low yields, as was also observed by Stoddart and co-workers in a related example.[12] Thus, under our conditions, saturated dimer **10** was obtained in a yield of 92%. Its Birch reduction yielded fully deprotected **4** in a yield of 96% and an overall yield of 29% from β-CD (Scheme 2).

Protected dimeric diol **10** was then used for the synthesis of **5**. Bis-*O*-alkylation of the two primary alcohols with **7** gave **11** in a yield of 93%. Ring-closing metathesis and saturation of the double bond by diimide reduction afforded **12** in a yield of 65% over two steps. Full deprotection was finally achieved by Birch reduction in a yield of 85% and **5** was obtained in an overall yield of 18% from β-CD in nine steps (Scheme 3).

These two syntheses illustrate the efficiency of our strategy, which not only provides a practical access to selectively modified CDs, but also allows the use of standard high-yielding reactions in common solvents thanks to the presence of the benzyl groups. Having hydrophilic dimers **4** and **5** in hand, we then studied their complexation and cross-linking properties.

Experimental investigation of the complexation properties of 4 and 5 towards ADAc and AD-chitosan

Interaction with ADAc: The inclusion of ADAc in the cavities of **4** and **5** was investigated by isothermal titration calorimetry (ITC). Data obtained were compared with data for **2** and **3** to clarify the role of bridging CD units on the binding mechanism.

The dependence of heat evolved upon titration of dimeric species **4** and **5** by a solution of ADAc (Figure 2) yielded an overall stoichiometry of 1.64 and 2.03, respectively, consistent with a 2:1 stoichiometry of binding (see Table 1).

These values are in sharp contrast with the values close to 1 found for dimeric species **2** and **3**, which were attributed

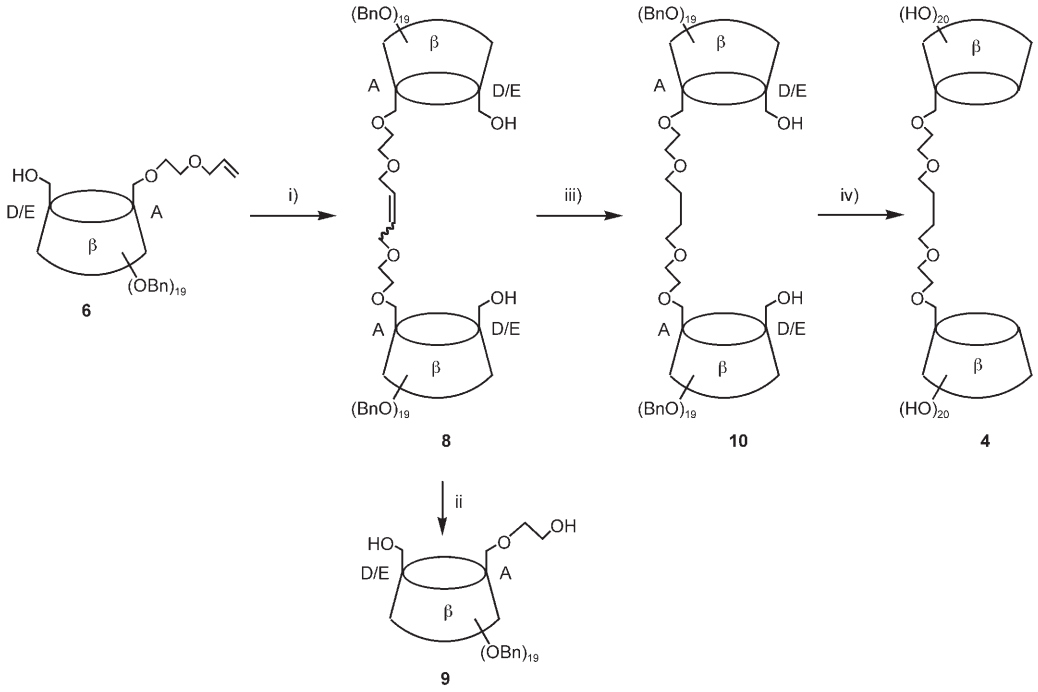

Scheme 2. Synthesis of dimer **4**. Reagents and conditions: i) $[Cl_2(PCy_3)_2Ru{=}CHPh]$ (5 mol%), CH_2Cl_2 (10^{-1} M), reflux, 15 h, then $Pb(OAc)_4$, RT, 3 h, 62%; ii) H_2, PtO_2, EtOAc, RT, 3 h; iii) NH_2NHTs, NaOAc, H_2O, ethylene glycol, reflux, 6 h, 92% ; iv) Na, liq. NH_3/THF (1:1), −33°C, 1 h, 96%.

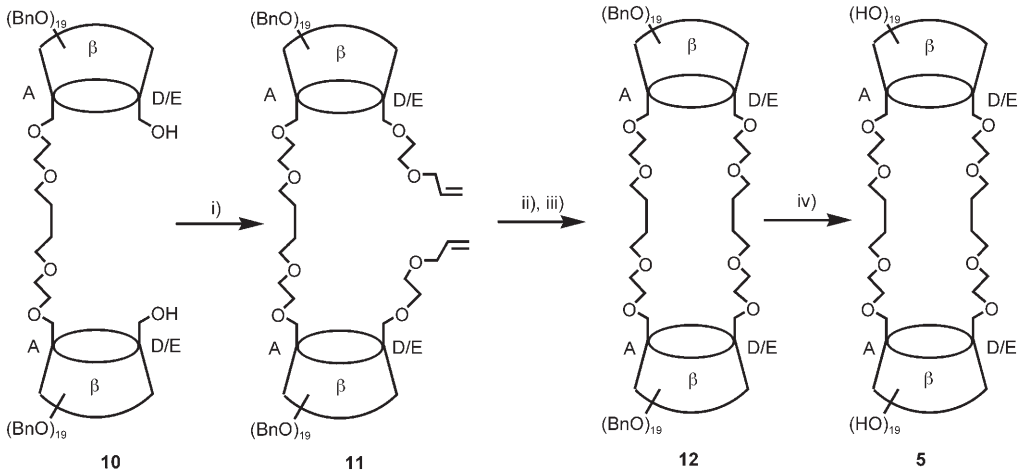

Scheme 3. Synthesis of duplex **5**. Reagents and conditions: i) **7**, NaH, nBu$_4$NI, THF, RT, 15 h, 93%; ii) [Cl$_2$(PCy$_3$)$_2$Ru=CHPh] (10 mol%), CH_2Cl_2 (10^{-3} M), reflux, 15 h, followed by Pb(OAc)$_4$, RT, 3 h, 85%; iii) NH_2NHTs, NaOAc, H_2O, ethylene glycol, reflux, 6 h, 77% ; iv) Na, liq. NH_3/THF (1:1), −33 °C, 1 h, 85%.

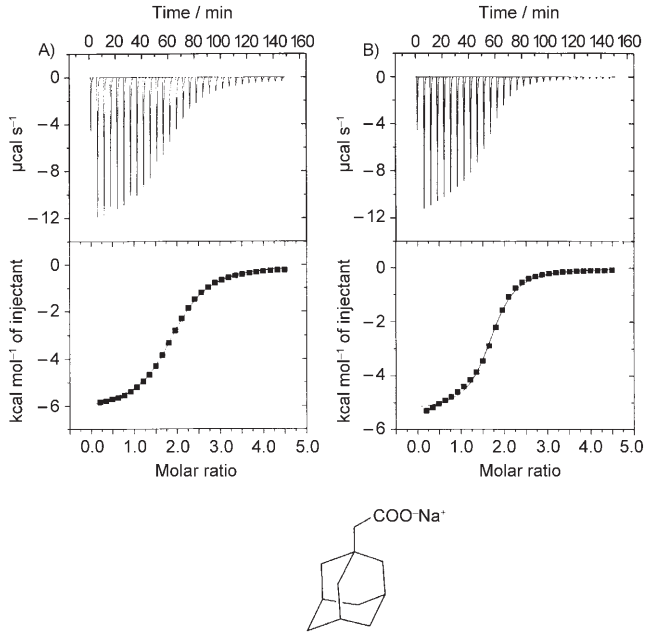

Figure 2. Calorimetric titration of A) dimer **4** and B) duplex **5** with ADAc in phosphate buffer (pH 7) at 25 °C. Top: Raw data for 30 sequential injections (10 µL per injection) of ADAc (7 mM) injected into the dimer solution (0.35 mM). Bottom: The integrated curve that shows the experimental points and the fit obtained by using the model based on a single set of identical binding sites for the titration of dimer **4** and duplex **5** with ADAc. The molecular structure of ADAc is also shown.

to the unavailability of about one half of the CD cavities owing to the formation of aggregates. It could thus be concluded from these data that the replacement of the aliphatic chains by oligo(ethylene oxide) spacers makes almost all of the CD cavities available for the inclusion of guest molecules. As can be seen from Figure 2A, the titration data for the ADAc/**4** system fitted perfectly with the simplest model in which a single set of identical binding sites is present. Comparison of the thermodynamic parameters for the binding of ADAc to **4** with those for ADAc binding to natural β-CD shows similar ΔH values, which suggests similar mechanisms of binding. However, the association constant for **4** is about a factor of two lower as a result of a less favourable entropy, as already found for **2**. Unlike the binding of ADAc to **4**, a model in which it was assumed that there were two sets of independent binding sites provided a better fit to the data obtained for the binding of ADAc to **5**, which suggests that the two binding sites do not behave identically. Nevertheless, owing to the uncertainties associated with the association constants and enthalpy values derived from this two-site model (six free parameters), comparison of the titration data with those of the other CD derivatives was performed by using the simplest model based on a single set of identical binding sites (see Table 1). It would appear that the apparent affinity of **5** for ADAc is somewhat higher than that of **4**, but much lower than that of **3**. Therefore, these results tend to confirm our previous assumption that the presence of the two octamethylene hydrophobic chains strengthens the hydrophobic interactions with hydrophobic adamantane. The ITC studies performed with ADAc as a model guest clearly demonstrate the availability of almost all of the CD cavities of the di-

Table 1. Thermodynamic parameters for the formation of inclusion complexes of ADAc with natural β-CD, β-CD dimers **2** and **4** and duplexes **3** and **5** derived from calorimetric titration experiments.

CD derivative	CD concn [mM]	ADAc concn [mM]	K_a [10^4 M^{-1}]	ΔH [kJ mol^{-1}]	$T\Delta S$ [kJ mol^{-1}]	n[b]
natural β-CD[a]	0.56	6.59	7.96 ± 0.05	−26.2 ± 0.04	1.76 ± 0.043	0.90 ± 0.01
2[a]	0.6	7.2	2.32 ± 0.07	−25.0 ± 0.4	−0.09 ± 0.407	1.02 ± 0.01
3[a]	0.6	4.4	26.42 ± 0.5	−28.2 ± 0.4	2.73 ± 0.403	0.80 ± 0.01
4	0.35	7	3.60 ± 0.06	−26.2 ± 0.06	−0.198 ± 0.073	1.64 ± 0.003
5	0.35	7	6.38 ± 0.50	−20.11 ± 0.2	7.29 ± 0.279	2.03 ± 0.01

[a] Data from ref. [9]. [b] n is the number of ADAc molecules per CD derivative.

meric species connected by hydrophilic oligo(ethylene oxide) spacers, as expected. On the other hand, they did not show the formation of strong complexes, as previously observed with **3**.

Interaction with AD-chitosan: As a result of the differences observed in the inclusion properties of the dimer and duplex by ITC, it was interesting to compare their ability to physically cross-link chitosan that possessed pendant adamantane groups by viscosity measurements. Viscosity measurements were performed by keeping the polymer concentration C constant ($0.6 \leq C\ [g\,L^{-1}] \leq 6$), whereas progressively increasing the concentration of **4** or **5**. Figure 3 displays the dependence on the [CD]/[AD] ratio of the zero-shear viscosity of AD-chitosan solutions at different concentrations. A viscosity enhancement can be noticed for **5** with AD-chitosan concentrations greater than $0.6\,g\,L^{-1}$, which indicates that interchain bridging can only be effective at concentrations greater than the polymer overlap concentration C^* ($\approx 0.9\,g\,L^{-1}$), as already observed.[9] On the other hand, there is no clear increase in the viscosity for **4**, although its ability to bind with ADAc is only slightly lower than that of **5**.

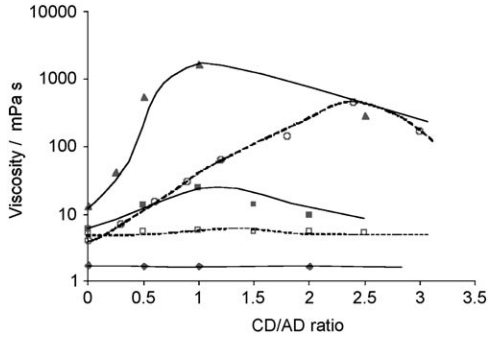

Figure 3. Variation of the viscosity of solutions of AD-chitosan in the concentration range of 0.6 to $6\,g\,L^{-1}$ (0.3 M CH_3COOH/0.03 M CH_3COONa, 25 °C) with the [CD]/[AD] ratio (i.e., with increasing concentration of CD dimeric species **3**, **4** and **5**). ◆) **5**/AD-chitosan ($0.6\,g\,L^{-1}$), ■) **5**/AD-chitosan ($3\,g\,L^{-1}$), ▲) **5**/AD-chitosan ($6\,g\,L^{-1}$), □) **4**/AD-chitosan ($3\,g\,L^{-1}$) and ○) **3**/AD-chitosan ($2.5\,g\,L^{-1}$).

Thus, these results emphasise the effect of double bridging, and consequently molecular rigidity, of the CD duplex on its ability to cross-link AD-chitosan chains with respect to binding affinity. Another important point is the position of the maximum viscosity with respect to the [CD]/[AD] ratio in the case of the duplexes **5** and **3**. The decrease in viscosity above the optimal [CD]/[AD] ratio was previously attributed to an increase of CD duplex monocomplexation to the detriment of dicomplexation owing to the presence of excess CD. The fact that this optimal [CD]/[AD] ratio is close to 1 for **5** and close to 2.5 for **3** probably reflects the percentage of available CD cavities, which is almost 100% for **5** and only 50% for **3**. Hence, it is necessary to add more of **3** to obtain maximum viscosity. On the other hand, the greater ability of **3** to enhance the solution viscosity of AD-chitosan might be partly explained by the greater strength of binding of its CD cavities with adamantane than for **5**.

The complexation of AD-chitosan by dimeric species **3**, **4** and **5** was also studied by calorimetric titration of the polymer by the CD derivatives in the dilute regime, as the high viscosity of the solutions above the overlap concentration of AD-chitosan precluded ITC measurements. The raw ITC data were treated by using the simplest model based on a single set of identical binding sites, with individual adamantane groups considered to bind to individual, discrete CD cavities (see Figure 4).[13] The enthalpy values are given in Table 2 for comparison, based on the assumption that these values are constant regardless of the stoichiometry. Table 2 also includes $K_{apparent}$ values, which have to be considered carefully as the stoichiometry of the complexes is changing

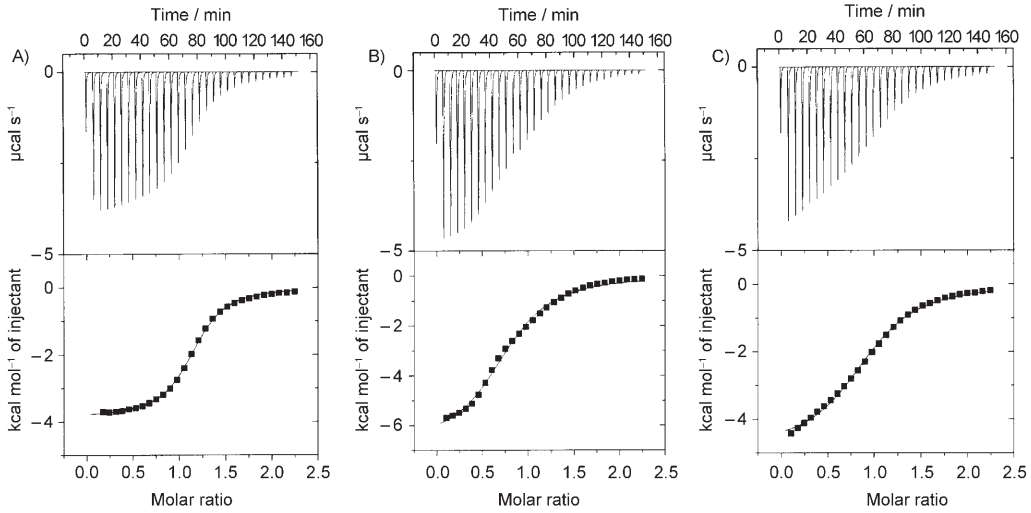

Figure 4. Calorimetric titration of AD-chitosan with A) **3**, B) **4** and C) **5** in 0.3 M CH_3COOH/0.03 M CH_3COONa at 25 °C. Top: Raw data for 30 sequential injections (10 µL per injection) of the solutions of dimeric species injected into the polymer solution. Bottom: The integrated curve that shows the experimental points and the fit obtained by using the model based on a single set of identical binding sites by considering individual adamantane groups binding to individual, discrete CD cavities.

Table 2. Thermodynamic parameters for the formation of inclusion complexes of natural β-CD and β-CD dimeric species **3**, **4** and **5** with AD-chitosan derived from calorimetric titration experiments.[a]

	CD cavity concn [mM]	ADAc concn [mM]	ΔH [kJ mol^{-1}]	$K_{apparent}$ [10^4 M^{-1}]
β-CD	3.5	0.35	-24.25 ± 0.03	6.17 ± 0.05
3	3.5	0.35	-16.12 ± 0.05	10.51 ± 0.32
4	3.5	0.35	-28.12 ± 0.53	2.78 ± 0.21
5	3.5	0.35	-20.24 ± 0.22	2.72 ± 0.13

[a] Calculations were performed by using the "one set of binding sites" model in which individual adamantane groups are considered to bind to individual, discrete CD cavities.

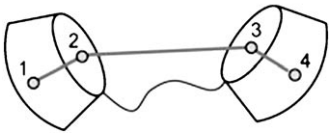

Figure 5. Schematic representation of a dimer of CD along with definitions of the relevant global conformational parameters. Positions 1–4 correspond to the centres of mass of the two CDs. 1: Centre of mass of the O2 and O3 atoms of CD1, 2: centre of mass of the C6 atoms of CD1, 3: centre of mass of the O2 and O3 atoms of CD2, 4: centre of mass of the C6 atoms of CD2, $D_{2\text{-}3}$ = distance between the two CDs, $\tau 1$ = orientational angle ∢1-2-3 and $\tau 2$ = orientational angle ∢2-3-4.

continuously. A detailed interpretation of the resulting thermodynamic data based on a theoretical model[14] could not be performed owing to the complexity of the guest and the multiple modes of association. However, some trends could be drawn from these results. The similar values of ΔH given in Table 1 and Table 2 for **4** and **5** clearly show the establishment of specific interactions between AD-chitosan and the dimeric species. Moreover, it can be seen from Figure 4 that for **3**, the magnitude of the released heat is nearly constant for the first injections in which adamantane is almost completely bound to the CD cavity. Then, compared with the titration with dimeric species **4** and **5**, it decreases rapidly until the last injection, which corresponds to the almost complete complexation of adamantane. This suggests a more efficient binding of grafted adamantane to **3** compared with the oxygenated species **4** and **5**, which seems to be supported by the $K_{apparent}$ values, although one has to be careful regarding these values, as mentioned above.

These studies clearly show the importance of double bridging for the efficient cross-linking of AD-chitosan chains. This property also appears to be linked to the difference in the affinity of the dimeric species for ADAc or AD-chitosan. Also, duplex **5** exhibited peculiar behaviour in which the two cavities seemed to behave differently. We therefore decided to broaden our investigations by using computational studies.

Computational studies: As a result of the close relationship between the structure and efficiency of binding or cross-linking, the molecular flexibility and accessibility of the CD cavities of the different dimeric species were initially examined. Our objective was to gain insights into the various accessible forms of these dimeric species.

In the first step, we generated an ensemble of 10000 different stable conformations for molecules **2** to **5** by using Monte Carlo and optimisation procedures. To characterise the various accessible forms of the molecules, the three conformational parameters presented in Figure 5 were defined. The inter-CD distances ($D_{2\text{-}3}$) vary from 4 to 16 Å with a maximum distribution around the average value of 10 Å. The two τ angles describe the angular orientation of the two CDs with respect to the principal axis of the molecule. The whole angular domain (0–180°) was explored in which maximum distributions occurred at 0, 90 and 180°.

The values of the τ angles are directly related to the accessibility of the cavities; the cavity is accessible when τ is close to 90 or 180° because the O2–O3 face of the CD is oriented outwards, whereas the cavity is not accessible when τ is close to 0° because the O2–O3 face of the CD is oriented inwards. All of the dimeric species are thus able to adopt many different conformations. However, the singly linked dimers are more flexible than the duplexes, as suggested by the larger distributions of the conformational parameters (data not shown).

Each ensemble of 10000 conformations was then divided into three conformational families that had two, one or no available cavities for adamantane inclusion. Figure 6 gives a graphical representation of representative molecular models of each family for **5**.

Interestingly, the relative orientations of the two CDs strongly resemble the different packing schemes of the native CDs in their crystal structures:[15] a cage-type arrangement (model A′ with $\tau 1 \approx 180°$ and $\tau 2 \approx 90°$) and channel or layered-type arrangements (head-to-head model A with $\tau 1 \approx 180°$ and $\tau 2 \approx 180°$, head-to-tail model B with $\tau 1 = 180°$ and $\tau 2 = 0°$ and tail-to-tail model C with $\tau 1 \approx 0°$ and $\tau 2 \approx 0°$). It can thus be concluded that the linkers are long enough to allow an unperturbed interaction between the CDs.

Only the lowest-energy conformation of each family was then considered for molecular dynamics experiments. After the equilibration period, structures A, B and C remained in their equilibrium geometry to retain the initial accessibility of their cavities and no major conformational interconversion was observed. Structure A′ converts rapidly into structure A. Calculated equilibrium potential energies are given in Table 3. According to these experiments, the preferred forms of the duplexes have two available cavities, whereas the preferred forms of the dimers have only one available cavity. The variation in energy associated with the transition between two-to-one available cavities indicated that the energy associated with the obstruction of a cavity is unfavourable for **3** and **5** ($+5.4$ and $+2.1$ kcal mol^{-1}), whereas it is favourable for **2** and **4** (-15.3 and -2.5 kcal mol^{-1}). A very small energy difference, within the borders of standard deviation, suggests that the two conformations are in equilibrium, whereas large values suggest a conformational preference. The obstruction of the second cavity when the first

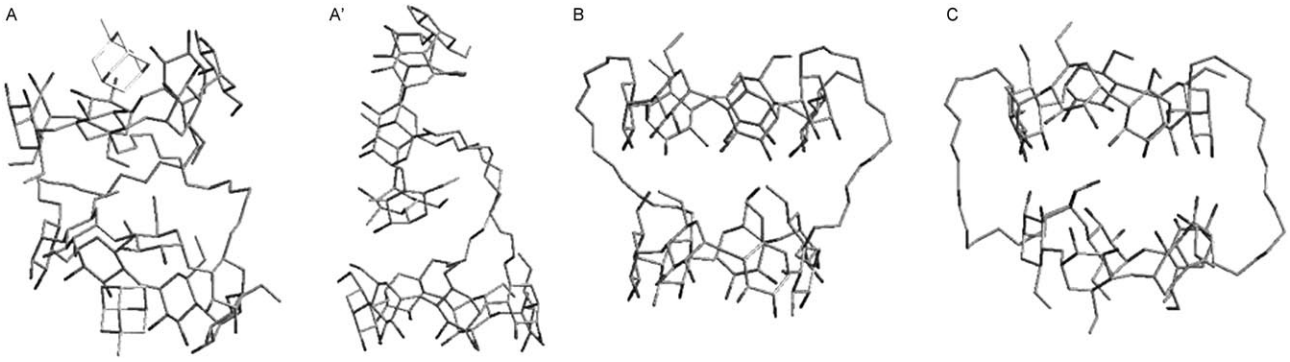

Figure 6. The different conformational families of **5**, which is used as a representative example. Models A and A′ have two available cavities; the inclusion complex with two adamantane molecules is shown in A. Conformation B has only one available cavity and conformation C has no available cavities. Hydrogen atoms have been omitted for clarity

Table 3. Average energies [kcal mol^{-1}] of the three conformational families of each molecule, which have none, one and two cavities available for the inclusion process.

	2	**3**	**4**	**5**
0 cavities	311±1	365±2	318±2	361±2
1 cavity	301±3	347±2	306±2	343±2
2 cavity	316±2	341±2	309±1	341±2
E_i non-sp[a]	−3±2	−6±3	−4±2	−6±3
$E_i(1)$[a]	−17±1	−14±1	−14±1	−10±1
$E_i(2)$[a]	−17±2	−16±2	−15±1	−15±1
RMSD-F	1.14±0.32	1.35±0.25	0.77±0.30	0.61±0.17
RMSD-C	0.77±0.20	1.09±0.28	0.63±0.25	0.73±0.15

[a] E_i non-sp: non-specific adsorption of the adamantane molecule, $E_i(1)$ interaction energy with the first adamantane molecule introduced and $E_i(2)$ interaction energy with the second adamantane molecule.

one was already obstructed was systematically found to be unfavourable. The effect of the hydrophilic/hydrophobic character of the spacers between the CDs on the energies is noticeable: molecules **2** and **3**, which possess one or two hydrophobic spacers, have one preferred conformation (large $\Delta E_{2cav\rightarrow1cav}$), whereas molecules **4** and **5**, which possess one or two hydrophilic spacers, have two conformations in equilibrium (small $\Delta E_{1cav\rightarrow2cav}$).

Another interesting fact provided by the models concerns the oxygen atoms of the two arms that seem to interact through hydrogen bonds with the hydroxymethyl groups of the CD. This feature usually contributes significantly to the enhancement of the rigidity of the CD rings.

Conformational analysis of the isolated species shows that they can adopt a wide variety of shapes; the two CD cavities are accessible in some of them, whereas folding of the molecule results in the obstruction of one or two cavities in the other conformations. An intrinsic mechanism for cavity obstruction is thus proposed. It is therefore not surprising that the experimental stoichiometries are quasi-systematically lower than the ideal 2:1 value. In addition, computational studies have clearly demonstrated that the flexibility of the whole molecule is influenced by the number and nature of the spacers. Although globally flexible, the doubly linked duplexes are more constrained than the singly bridged dimers. Modelling results support the intuitive idea that the number of allowed conformations is limited for the doubly bridged species and consequently that this structural feature is likely to play a significant role in the interaction processes. Furthermore, the most stable conformations possess two available cavities in the cases of the duplexes, whereas the dimers are more stable in a conformation in which only one cavity is available. This observation gives some explanation for the difference in behaviour in the cross-linking experiments.

In the next step, the complexation mechanism of the dimeric species was investigated. Molecular dynamics experiments were performed upon the sequential introduction of a first and a second adamantane molecule for all of the conformations considered in the preceding section. The energies for both the adsorption and inclusion phenomena for all of the dimeric species are given in Table 3. Unsurprisingly, as solvation effects were modelled by using a simple dielectric constant, there are discrepancies between the experimental enthalpy values and those derived from modelling experiments. The enthalpies of inclusion of the dimeric derivatives are consistent with our preliminary molecular dynamics simulations on a simple CD interacting with an adamantane molecule, which gave an average inclusion enthalpy of -15 ± 2 kcal mol^{-1}. Interesting information could, however, be obtained by comparing the calculated values. The equilibrium enthalpies of inclusion for dimers **2** and **4** and for duplex **3** are almost the same for both cavities, which suggests that their two sites are identical. In contrast, for **5**, the inclusion of two molecules of adamantane involves different enthalpy values. We have thus rationalised here the observation made in the ITC experiments that complexation of ADAc by **5** did not perfectly fit the model of two identical binding sites.

As a result of the differences in the chemical structures of the four dimeric species, together with the strong interactions that take place between the CD and adamantane molecules, one should observe significant differences in the motional freedom of the CD rings in the free or complexed states. This influence can be easily shown by comparing the root-mean-square deviation (RMSD) of the coordinates of the heavy atoms of the CDs (except the O6 atoms) of the

dimeric derivatives in the two states: in the absence of adamantane molecules (RMSD-F) and in the presence of adamantane molecules included in the cavities (RMSD-C). The RMSD values given in Table 3 reveal a general significant restriction of the motional freedom of the CDs in the dimeric species, which suggests an unfavourable entropic cost associated with the inclusion of adamantane in the CD cavity. Duplex **5** behaves differently because the inclusion of adamantane has a limited effect on the RMSD values; it appears to be entropically favourable in contrast to the other dimeric species.

The entropy of interaction with adamantane is correlated with the flexibility of the CD macro-rings, which is generally affected by the absence or by the presence of adamantane molecules. Inclusion is generally associated with a significant restriction of the motional freedom of the CD molecule and thus results in an unfavourable entropy, which is the case with **2**, **3** and **4**. However, conformational analysis of **5** reveals that the oxygen atoms of its spacers can interact with the secondary hydroxy groups of the CDs. This conformational hindrance would result in both a small distortion and rigidity of the CDs. As a consequence its interaction with adamantane is weaker, which explains the smaller experimental enthalpies of inclusion, and on the other hand, adamantane inclusion is facilitated by a better entropy of inclusion, qualitatively rationalised by the initial rigidity of the molecule (see Table 1).

Computational studies have given us a better understanding of the stoichiometry of complexation through conformational analysis. In addition, hydrogen-bond formation between the primary hydroxy groups of the CDs and the oxygen atoms of the inter-CD bridges has been suggested, which might account for the particular behaviour of **5** regarding the enthalpy and entropy of complexation. We have thus confirmed the ITC observation that **5** possesses two cavities that behave differently, although a clear mechanism could not be proposed. Finally, the modelling study could not account for the unexpected behaviour of **3**, in particular, its unusual association constant with adamantane. This is likely to be related to the fact that the study was performed in a dielectric medium to mimic solvation.

Conclusion

Efficient syntheses of two new hydrophilic dimeric β-CD derivatives, dimer **4** and duplex **5**, were developed for their subsequent study as non-covalent cross-linking agents of a biopolymer. ITC studies by using ADAc as a model guest clearly demonstrated the availability of almost all of the CD cavities of these dimeric species, contrary to their counterparts that possess octamethylene arms. As already observed with the latter, the ability of the hydrophilic dimeric derivatives to cross-link AD-chitosan chains was shown to be closely related to their molecular architecture. Duplex **5** appeared to be more efficient at physically cross-linking the biopolymer in a semi-dilute regime. However, comparison with duplex **3** indicated that **3** induces higher viscosity enhancements, but at higher concentrations. Computational studies clearly confirm the importance of double bridging for the rigidity of the structure, and hence, its ability to cross-link the biopolymer. It is foreseeable that duplex structures combining the advantages of these two derivatives, that is, their higher affinity for adamantane and the hydrophilicity of the inter-CD links, should be promising candidates for cross-linking agents. We are now working in this direction.

Experimental Section

Materials: AD-chitosan with a degree of substitution equal to 0.05 was synthesised as previously reported.[16] The parent chitosan used has a weight-average molecular weight M_w of 195000 and is a commercial sample from Pronova (Norway) with a degree of N-acetylation equal to 0.12. The overlap concentration C^*, which characterises the transition from the dilute concentration regime to the semi-dilute one, is around 0.9 g L^{-1} for this chitosan sample.[16] β-CD dimeric species **2** and **3** were synthesised as described in detail elsewhere.[8] β-CD was supplied by Cyclolab (Budapest, Hungary). All other chemical products and reagents were purchased from Fluka (Buchs, Switzerland).

Elemental analysis and optical rotation measurements: Elemental analyses were performed by Service de Microanalyse, CNRS ICSN, Av. de la Terrasse, 91198 Gif-sur-Yvette Cedex (France). Optical rotation was measured at 20±2°C with a Perkin–Elmer Model 241 digital polarimeter by using a 10 cm, 1 mL cell.

NMR spectroscopy: ^{1}H NMR spectra were recorded with a Bruker DRX 400 spectrometer for solutions in $CDCl_3$ or D_2O at ambient temperatures. Assignments were made by using COSY experiments. ^{13}C NMR spectra were recorded at 100.6 MHz with a Bruker DRX 400 spectrometer for solutions in $CDCl_3$ or D_2O by using 77.00 ppm as the central line of $CDCl_3$. Assignments were made on the basis of the J-mod technique and HMQC experiments.

Mass spectrometry: Fast atom bombardment mass spectra (FAB-MS) were obtained with a JMS-700 spectrometer. MALDI-TOF mass spectra were recorded with a PerSeptive Biosystems Voyager Elite (Framingham MA, USA) time-of-flight mass spectrometer. This instrument was equipped with a nitrogen laser (337 nm), delayed extraction and a reflector. PEG standards were used to calibrate the mass scale by using the two point calibration software 3.07.1 from PerSeptive Biosystems. The matrix, 2,5-dihydroxybenzoic acid (2,5-DHB) was obtained from Sigma (France) and used without further purification. ESI mass spectra were recorded with a Q-TOF1 (Micromass) time-of-flight mass spectrometer with a sample cone of 40 V.

Titration calorimetry: ITC was performed by using a Microcal VP-ITC titration microcalorimeter (Northampton, USA). In individual titrations, injections of ADAc (10 μL) were added from a computer-controlled 300 μL microsyringe at intervals of 5 min to solutions of the β-CD dimeric species **4** and **5** (cell volume = 1.4478 mL) that contained the same solvent as ADAc (phosphate buffer, pH 7) with stirring at 297 r.p.m. at 25°C. The observed heat effects on injection of ADAc into a cell that contained only the solvent under identical conditions were identical to the heat signals at the end of the titration after saturation was reached. The raw experimental data were presented as the amount of heat produced after each injection of ADAc as a function of time. The amount of heat produced per injection was calculated by integration of the area under individual peaks by the instrument software after taking into account heat of dilution. The experimental data were fitted to a theoretical titration curve by using the instrument software (ORIGIN software, Microcal), in which ΔH (the enthalpy change in kJ mol^{-1}), K_a (the association constant in M^{-1}) and n (complex stoichiometry) were adjustable parameters. In all cases, calculations were performed by using the "one set

of binding sites" model. The $T\Delta S$ values were calculated from the equation $\Delta G=\Delta H-T\Delta S=-RT\ln K_a$, in which ΔG, ΔH and ΔS are the changes in free energy, enthalpy and entropy of binding, respectively, T is the absolute temperature and $R=8.314\,J\,K^{-1}\,mol^{-1}$. Consequently, the standard errors for the $T\Delta S$ values depend on those for T, ΔG and ΔH (which are adjustable parameters together with n). They were calculated as described in the literature.[17]

Viscometry: The steady shear flow properties of solutions of adamantane-chitosan in the absence and in the presence of CD dimeric species **4** or **5** were measured by using a low-shear viscometer (LS30 from Contraves) or a cone-plate rheometer (ARES-RFS from TA Instruments) depending on the sample viscosity. In the latter case, the cone used had a diameter of 5 cm and an angle of 0.04 rad, and experiments were carried out with a film of silicone to avoid solvent evaporation. The solutions of AD-chitosan and CD-derivatives **4** and **5** were prepared separately in 0.3 M CH_3COOH/0.03 M CH_3COONa, which is a good solvent of chitosan. The dissolution time for adamantane-chitosan was at least 1 d at room temperature. The CD dimeric species were dissolved in the minimum amount of solvent (65 mg mL^{-1} for **4** and 70 mg mL^{-1} for **5**) to avoid dilution of the polymer solution after their addition under stirring. After each addition, the samples were allowed to rest for at least 1 h before measurements were taken.

Molecular modelling

Force field: All calculations were performed with the modelling package Cerius^2 molecular modelling program.[18] Unless otherwise noted we used the default setup. The consistent valence force field cvff(91) parameter set was applied.[19] This force field employs terms for the bond lengths, the bond angles and the torsional potentials for the bonded terms of the potential energy function. It employs a van der Waals potential and an electrostatic potential for the non-bonded terms. A Morse potential was used for the bond length terms, a quadratic potential for the bond angle terms and a single cosine form for the torsional term. A Lennard-Jones function was used for the van der Waals term and a coulombic form for the electrostatic term. The charge equilibration approach[20] was used to evaluate point charges on every atom. The dielectric constant used to calculate the electrostatic interactions was set to 80 to mimic a hydrated environment.

Minimisation, Monte Carlo and dynamics: Dimeric species **2**–**5** were generated from the coordinates of the crystal structure of β-CD[21] and from graphical constructions of the spacers and adamantane molecule by using standard geometries for bond lengths and bond angles. A Monte Carlo procedure was then used to sample the conformational space of the molecules in isolation. A total of 10000 conformations were generated by attribution of random values (between 0 and 360°) of the torsion angles of the spacers and of the hydroxy and hydroxymethyl groups of the CDs. Each conformation was then minimised. Molecular dynamics experiments were carried out in the NVT ensemble. The equations of motion were solved by using the Verlet algorithm[22] with a time step of 1 fs. The lengths of the MD simulations varied from 500 ps to 1 ns (the first 200 ps were reserved for the equilibration of the system). To maintain the average temperature at 300 K, the velocities of the particles were rescaled. Random velocities were assigned to the atoms, which correspond to a Boltzmann distribution at 300 K. The Monte Carlo conformational sampling was then divided into three conformational families that had 2, 1 and 0 accessible cavities. The lowest-energy structure of each family of each molecule was then used for further molecular dynamics experiments. Molecular dynamics studies were performed on 1) the dimeric species alone, 2) the dimeric species in the presence of 1-methyladamantane and 3) the dimeric species in the presence of a second 1-methyladamantane molecule (the first one was studied in the preceding calculation). In this study, we only wanted to focus on the inclusion of adamantane in the CD cavities induced by hydrophobic interactions. Therefore, we selected the methyl derivative of adamantane instead of the carboxylate derivative that was studied experimentally. As a matter of fact, the magnitude of the electrostatic interactions is considerably larger than the van der Waals interaction, so the carboxylate–hydroxy interactions might mask the hydrophobic interactions that occur between the adamantane moiety and the cavity of the CD.

Synthesis: Reactions were monitored by thin-layer chromatography (TLC) on a precoated plate of silica gel 60 F_{254} (layer thickness 0.2 mm; E. Merck, Darmstadt, Germany) and detected by charring with sulfuric acid. Flash column chromatography was performed on silica gel 60 (230–400 mesh, E. Merck).

Dimer 4: Dimer **10** (200 mg, 34 μmol) was dissolved in a mixture of THF/NH_3 (1:1, 20 mL) at −78 °C. Small pieces of Na (300 mg, excess) were then added. The blue solution was heated at reflux for 1 h (−33 °C), carefully quenched with *i*PrOH (20 mL) and concentrated. A solution of the residue in water (15 mL) was neutralised with IR-120 H^+ resin, diluted with EtOAc (15 mL), stirred vigorously for 30 min and filtered. The organic layer was separated, extracted with water (3×10 mL) and the combined aqueous layers were concentrated. The residue was purified by column chromatography on a Sephadex G25 column (water) to give **4** (82 mg, 96 %) as a white powder. $[\alpha]_D^{20}=+132$ ($c=1.0$ in H_2O); ^{1}H NMR (400 MHz, D_2O): $\delta=1.55$–1.70 (m, 8H; 8×$OCH_2CH_2CH_2CH_2O$), 3.32–4.12 (m, 152H; 98×CH, 38×OH, 16×OCH_2CH_2O), 5.01–5.12 ppm (m, 14H; 14×1-H); ^{13}C NMR (100 MHz, D_2O): $\delta=25.6$–26.3 (CH_2), 60.3–61.3 (OCH_2), 69.0–70.6 (OCH_2), 70.7–70.9 (CH), 71.0–71.4 (OCH_2), 72.1–72.6 (CH), 73.3–73.5 (CH), 81.0–82.5 (CH), 101.6–102.7 ppm (CH); MS (MALDI-TOF): m/z (%): 2434.15 (100) [M^+−Na].

Duplex 5: Duplex **12** (214 mg, 36 μmol) was dissolved in a mixture of THF/NH_3 (1:1, 20 mL) at −78 °C. Small pieces of Na (350 mg, excess) were then added. The blue solution was heated at reflux for 1 h (−33 °C), carefully quenched by *i*PrOH (20 mL) and concentrated. A solution of the residue in water (15 mL) was neutralised with IR-120 H^+ resin, diluted with EtOAc (15 mL), stirred vigorously for 30 min and filtered. The organic layer was separated, extracted with water (3×10 mL) and the combined aqueous layers were concentrated. The residue was purified by column chromatography on a Sephadex G25 column (water) to give **5** (78 mg, 85 %) as a white powder. ^{1}H NMR (400 MHz, D_2O): $\delta=1.55$–1.70 (m, 8H; 8×$OCH_2CH_2CH_2CH_2O$), 3.32–4.12 (m, 152H; 98×CH, 38×OH, 16×OCH_2CH_2O), 5.01–5.12 ppm (m, 14H; 14×1-H); ^{13}C NMR (100 MHz, D_2O): $\delta=25.6$–26.3 (CH_2), 60.3–61.3 (OCH_2), 69.0–70.6 (OCH_2), 70.7–70.9 (CH), 71.0–71.4 (OCH_2), 72.1–72.6 (CH), 73.3–73.5 (CH), 81.0–82.5 (CH), 101.6–102.7 ppm (CH); MS (MALDI-TOF): m/z (%): 2575.24 (100) [M^+−Na].

Monomer 6: $n$$Bu_4NI$ (159 mg, 0.39 mmol) and KH (315 mg, 2.36 mmol, *w*/*w* 30 % in oil) were added to a solution of **1** (5.6 g, 1.97 mmol) in THF (179 mL) at 0 °C under argon. The reaction mixture was stirred at 0 °C under argon for 20 min before **7** (604 mg, 2.36 mmol) was added. The reaction mixture was stirred at RT under argon for 18 h, then treated with MeOH (25 mL) and the solvent was evaporated. The residue was diluted with CH_2Cl_2 (70 mL) and treated with a saturated solution of NH_4Cl (40 mL). The layers were separated and the aqueous layer was extracted with CH_2Cl_2 (3×50 mL). The organic layers were combined, washed with brine, dried with $MgSO_4$, filtered and concentrated. The residue was purified by column chromatography on silica gel (cyclohexane/EtOAc, 4:1 then 3:1) to give **6** (3.88 g, 67 %) as a white foam. $R_f=0.44$ (cyclohexane/EtOAc 3:1); ^{1}H NMR (400 MHz, $CDCl_3$): $\delta=3.40$–3.75 (m, 18H; 7×2-H, 7×6-H, 4×CH_2O), 3.82–4.12 (m, 30H; 7×3-H, 7×4-H, 7×5-H, 7×6-H, 2×$OCH_2CH{=}CH_2$), 4.35–4.60 (m, 22H; 22×CHPh), 4.66–4.85 (m, 10H; 10×CHPh), 4.95–5.45 (m, 14H; 7×1-H, 6×CHPh, 2×$OCH_2CH{=}CH_2$), 5.87 (ddt, $^3J_{trans}=23.0$ Hz, $^3J_{cis}=11.3$ Hz, $^3J=5.7$ Hz, 1H; $OCH_2CH{=}CH_2$), 7.18–7.32 ppm (m, 95H; CH arom.); ^{13}C NMR (100 MHz, $CDCl_3$): $\delta=26.9$ (CH_2), 68.6–69.3 (CH_2), 70.5 (CH_2), 71.3–71.8 (CH), 71.9–72.2 (CH_2), 72.4–72.9 (CH_2), 73.2–73.3 (CH_2), 74.7–75.9 (CH_2), 77.4–78.0 (CH), 78.6–79.9 (CH), 80.7–81.2 (CH), 97.9–98.8 (C-1), 116.9 ($OCH_2CH{=}CH_2$), 127.3–128.3 (CH arom.), 134.8 ($OCH_2CH{=}CH_2$), 137.8–138.5 (C arom. quat.), 138.8–139.4 ppm (C arom. quat.); MS (FAB): m/z (%): 2954.4 (100) [M^+−Na]; elemental analysis calcd (%) for $C_{180}H_{192}O_{36}$ (2931): C 73.75, H 6.60; found: C 73.35, H 6.46.

Dimer 10: A solution of **6** (1.38 g, 473 μmol) in CH_2Cl_2 (5.7 mL) was degassed three times with argon. Grubbs catalyst (19 mg, 24 μmol) was added and the reaction mixture was heated at reflux under argon for 15 h. $Pb(OAc)_4$ (16 mg, 36 μmol) was added at RT and the mixture was stirred for an additional 3 h under argon at RT before the solvent was evaporated. The residue was purified by column chromatography on

silica gel (cyclohexane/EtOAc, 4:1 then 3:1) to give **8** (844 mg, 62%) as a white foam. Dimer **8** (780 mg, 134 μmol) was dissolved in 1,2-dimethoxyethane (19.5 mL) and treated with *p*-toluenesulfonyl hydrazide (2.04 g, 10.9 mmol). The reaction mixture was heated at reflux and a solution of sodium acetate in water (1.85 g in 13 mL H_2O) was added dropwise. After heating at reflux for 6 h, the reaction mixture was concentrated, diluted in EtOAc (20 mL) and washed with H_2O (15 mL). The aqueous layer was extracted with EtOAc (3×15 mL). The organic layers were combined, washed with brine (40 mL), dried with $MgSO_4$ and concentrated. The crude product was purified by column chromatography on silica gel (cyclohexane/EtOAc, 4:1, then 3:1) to give **10** (717 mg, 92%) as a white foam. R_f=0.42 (cyclohexane/EtOAc 2:1); ^{1}H NMR (400 MHz, $CDCl_3$): δ=1.45–1.57 (m, 4H; 4×$OCH_2CH_2CH_2CH_2O$), 2.48 (br s; 2×OH), 3.31 (br d, J=4.2 Hz, 4H; 4×$OCH_2CH_2CH_2CH_2O$), 3.36–4.12 (m, 92H; 14×2-H, 14×3-H, 14×4-H, 14×5-H, 28×6-H, 8×OCH_2CH_2O), 4.32–4.60 (m, 46H; 46×CHPh), 4.62–4.83 (m, 19H; 19×CHPh), 4.90–5.02 (m, 7H; 7×CHPh), 5.03–5.27 (m, 15H; 10×1-H, 5×CHPh), 5.34–5.44 (m, 4H; 4×1-H), 7.10–7.30 ppm (m, 190H; CH arom.); ^{13}C NMR (100 MHz, $CDCl_3$): δ=26.1 (CH_2), 26.2 (CH_2), 26.8 (CH_2), 26.9 (CH_2), 69.2–69.7 (OCH_2), 70.4 (OCH_2), 71.0 (OCH_2), 71.1–71.9 (CH), 72.4–72.9 (CH_2Ph), 73.1–73.4 (CH_2Ph), 74.7–75.9 (CH_2Ph), 78.5–79.8 (CH), 80.7–81.1 (CH), 97.9–98.9 (C-1), 127.4–128.3 (CH arom.), 137.8–138.5 (C arom. quat.), 138.8–139.3 ppm (CH arom. quat.); MS (MALDI-TOF): m/z (%): 5855.4 (100) [M^+−Na]; elemental analysis calcd (%) for $C_{358}H_{382}O_{72}(H_2O)_2$ (5866): C 73.22, H 6.62; found: C 72.91, H 6.72.

Dimer 11: At 0°C and under argon, nBu$_4$NI (2.8 mg, 7.5 μmol) and NaH (60% dispersion in oil, 18 mg, 450 μmol) were added to a solution of **10** (436 mg, 75 μmol) in THF (3 mL). The reaction mixture was stirred at 0°C under argon for 20 min, then **7** (115 mg, 450 μmol) was added. The mixture was stirred at RT under argon for 15 h, then NaH (60% dispersion in oil, 18 mg, 450 μmol) and the **7** (115 mg, 450 μmol) were added. After 8 h, the reaction mixture was treated with MeOH (5 mL), evaporated and finally diluted with CH_2Cl_2 (15 mL). The organic layer was washed with a saturated solution of NH_4Cl (10 mL). The aqueous layer was extracted with CH_2Cl_2 (3×15 mL). The organic layers were combined, washed with brine (40 mL), dried with $MgSO_4$, filtered and concentrated. The crude mixture was purified by column chromatography on silica gel (cyclohexane/EtOAc, 6:1, then 3:1) to give **11** (417 mg, 93%). R_f=0.60 (cyclohexane/EtOAc 3:1, eluted twice); ^{1}H NMR (400 MHz, $CDCl_3$): δ=1.45–1.60 (m, 4H; 4×$OCH_2CH_2CH_2CH_2O$), 3.30–3.38 (m, 4H; 4×$OCH_2CH_2CH_2CH_2O$), 3.40–3.75 (m, 33H; 17×CH, 16×OCH_2CH_2O), 3.85–4.15 (m, 67H; CH), 4.40–4.62 (m, 52H; 52×CHPh), 4.78–4.87 (m, 12H; 12×CHPh), 5.00–5.35 (m, 30H; 14×1-H, 12×CHPh, 4×$OCH_2CH{=}CH_2$), 5.89 (dddd, $^3J_{trans}$=19.5 Hz, $^3J_{cis}$=10.5 Hz, ^3J=9 Hz, 2H; 2×$OCH_2CH{=}CH_2$), 7.12–7.30 ppm (m, 190H; CH arom.); ^{13}C NMR (100 MHz, $CDCl_3$): δ=26.2 (CH_2), 26.9 (CH_2), 29.7 (CH_2), 30.1 (CH_2), 68.9–69.7 (OCH_2), 70.3–70.5 (OCH_2), 70.9 (OCH_2), 71.2–71.6 (CH), 71.9–73.3 (CH_2Ph), 75.0–75.7 (CH_2Ph), 77.7–79.4 (CH), 80.7–80.9 (CH), 98.2–98.6 (C-1), 116.8, 116.85 ($OCH_2CH{=}CH2$), 127.3–128.3 (CH arom.), 134.7, 134.8 ($OCH_2CH{=}CH_2$), 138.1–138.4 (C arom. quat.), 139.1–139.3 ppm (CH arom. quat.); MS (MALDI-TOF): m/z (%): 6023.36 (100) [M^+−Na]; elemental analysis calcd (%) for $C_{368}H_{398}O_{74}(H_2O)_2$ (6036): C 73.16, H 6.71; found: C, 73.03, H 6.71.

Duplex 12: A solution of **11** (389 mg, 65 μmol) in CH_2Cl_2 (65 mL, 0.001 M) was degassed three times with argon. Grubbs catalyst (5.3 mg, 6.5 μmol) was added and the reaction mixture was heated at reflux under argon for 15 h. $Pb(OAc)_4$ (4.3 mg, 9.7 μmol) was added at RT and the mixture was stirred for an additional 3 h under argon at RT before the solvent was evaporated. The residue was purified by column chromatography on silica gel (cyclohexane/EtOAc, 4:1 then 2:1) to give an unsaturated duplex (327 mg, 85%) as a white foam. Duplex **11** (316 mg, 53 μmol) was dissolved in 1,2-dimethoxyethane (8 mL) and treated with *p*-toluenesulfonyl hydrazide (830 mg, 4.4 mmol). The reaction mixture was heated at reflux and a solution of sodium acetate in water (750 mg in 5.3 mL H_2O) was added dropwise. After heating at reflux for 6 h, the reaction mixture was concentrated, diluted in EtOAc (20 mL) and washed with H_2O (15 mL). The aqueous layer was extracted with EtOAc (3×15 mL). The organic layers were combined, washed with brine (40 mL), dried with $MgSO_4$ and concentrated. The crude was purified by column chromatography on silica gel (cyclohexane/EtOAc, 4:1) to give **12** (245 mg, 77%) as a white foam. R_f=0.57 (Cy/EtOAc 3:1); ^{1}H NMR (400 MHz, $CDCl_3$): δ=1.45–1.47 (m, 8H; 8×$OCH_2CH_2CH_2CH_2O$), 3.24 (t, 8H; 8×$OCH_2CH_2CH_2CH_2O$), 3.32–4.20 (m, 83H; 67×CH, 16×OCH_2CH_2O), 4.32–4.63 (m, 50H; 50×CHPh), 4.73–4.89 (m, 16H; 16×CHPh), 4.92–5.07 (m, 8H; 4×1-H, 4×CHPh), 5.09 (t, $^3J_{1,2}$=3.4 Hz, 2H; 2×1-H), 5.13 (t, $^3J_{1,2}$=3.3 Hz, 2H; 2×1-H), 5.22 (d, ^2J=10.5 Hz; 2×CHPh), 5.24 (d, ^2J=10.6 Hz; 2×CHPh), 5.34 (m, 4H; 2×1-H, 2×CHPh), 5.40 (t, $^3J_{1,2}$=3.3 Hz, 2H; 2×1-H), 5.44 (d, $^3J_{1,2}$=3.6 Hz, 1H; 1×1-H), 5.46 (d, $^3J_{1,2}$=3.7 Hz, 1H; 1×1-H), 7.05–7.30 ppm (m, 190H; CH arom.); ^{13}C NMR (100 MHz, $CDCl_3$): δ=26.2 (CH_2), 26.3 (CH_2), 69.1–69.4 (OCH_2), 70.2–70.9 (OCH_2), 71.2–71.7 (CH), 72.2–73.3 (CH_2Ph), 74.6–76.2 (CH_2Ph), 78.3–79.4 (CH), 80.4–81.0 (CH), 97.9–98.9 (C-1), 127.4–128.3 (CH arom.), 138.1–138.5 (C arom. quat.), 139.0–139.3 ppm (CH arom. quat.); MS (MALDI-TOF): m/z (%): 5999.8 (100) [M^+−Na]; elemental analysis calcd (%) for $C_{366}H_{396}O_{74}(H_2O)_2$ (6012): C 73.08, H 6.70; found: C 72.81, H 6.78.

Acknowledgements

The authors would like to thank Cyclolab (Hungary) for a generous supply of β-CD. M.S. would also like to personally thank Prof. Pierre Sinaÿ for his support.

[1] a) R. Breslow, S. Chung, *J. Am. Chem. Soc.* **1990**, *112*, 9659; b) R. Breslow, S. Halfon, B. Zhang, *Tetrahedron* **1995**, *51*, 377; c) R. Breslow, B. Zhang, *J. Am. Chem. Soc.* **1996**, *118*, 8495.
[2] M. R. de Jong, J. F. J. Engbersen, J. Huskens, D. N. Reinhoudt, *Chem. Eur. J.* **2000**, *6*, 4034.
[3] a) Y. Liu, B. Li, C. C. You, T. Wada, Y. Inoue, *J. Org. Chem.* **2001**, *66*, 225; b) Y. Liu, Y. Chen, S.-X. Liu, X.-D. Guan, T. Wada, Y. Inoue, *Org. Lett.* **2001**, *3*, 1657; c) Y. Liu, Y. Song, Y. Chen, X. Q. Li, F. Ding, R. Q. Zhong, *Chem. Eur. J.* **2004**, *10*, 3685; Y. Liu, H. M. Yu, Y. Chen, Y. L. Zhao, *Chem. Eur. J.* **2006**, *12*, 3858.
[4] a) F. Venema, H. F. M. Nelissen, P. Berthault, N. Birlirakis, A. E. Rowan, M. C. Feiters, R. J. M. Nolte, *Chem. Eur. J.* **1998**, *4*, 2237; b) F. Venema, A. E. Rowan, R. J. M. Nolte, *J. Am. Chem. Soc.* **1996**, *118*, 257.
[5] H. Yamamura, S. Yamada, K. Kohno, N. Okuda, S. Araki, K. Kobayashi, R. Katakai, K. Kano, M. Kawai, *J. Chem. Soc., Perkin Trans. 1* **1999**, 2943.
[6] I. Tabushi, Y. Kuroda, K. Shimokawa, *J. Am. Chem. Soc.* **1979**, *101*, 1614; R. Brelow, S. Chung, *J. Am. Chem. Soc.* **1990**, *112*, 9659; R. Breslow, S. Halfon, B. Zhang, *Tetrahedron* **1995**, *51*, 377; K. Sasaki, M. Nagasaka, Y. Kuroda, *Chem. Commun.* **2001**, 2630.
[7] a) T. Lecourt, A. J. Pearce, A. Herault, M. Sollogoub, P. Sinaÿ, *Chem. Eur. J.* **2004**, *10*, 2960; b) O. Bistri, P. Sinaÿ, M. Sollogoub, *Tetrahedron Lett.* **2005**, *46*, 7757; c) O. Bistri, P. Sinaÿ, M. Sollogoub, *Chem. Commun.* **2006**, 1112; d) O. Bistri, P. Sinaÿ, M. Sollogoub, *Chem. Lett.* **2006**, *35*, 534; e) O. Bistri, P. Sinaÿ, M. Sollogoub, *Tetrahedron Lett.* **2006**, *47*, 4137.
[8] T. Lecourt, J.-M. Mallet, P. Sinaÿ, *Eur. J. Org. Chem.* **2003**, 4553; O. Bistri, T. Lecourt, J.-M. Mallet, M. Sollogoub, P. Sinaÿ, *Chem. Biodiv.* **2004**, *1*, 129.
[9] T. Lecourt, P. Sinaÿ, C. Chassenieux, M. Rinaudo, R. Auzély-Velty, *Macromolecules* **2004**, *37*, 4635.
[10] T. Lecourt, J.-M. Mallet, P. Sinaÿ, *Tetrahedron Lett.* **2002**, *43*, 5533.
[11] M. Surzur, G. Torri, *Bull. Soc. Chim. Fr.* **1970**, 3070; M. Delgado, J. D. Martin, *J. Org. Chem.* **1999**, *64*, 4798.
[12] S.-H. Chiu, D. C. Myles, R. L. Garrell, J. F. Stoddart, *J. Org. Chem.* **2000**, *65*, 2792.
[13] J. B. Corbell, J. J. Lundquist, E. J. Toone, *Tetrahedron: Asymmetry* **2000**, *11*, 95.
[14] A. Mulder, J. Huskens, D. N. Reinhoudt, *Org. Biomol. Chem.* **2004**, *2*, 3409.
[15] K. Harata, *Chem. Rev.* **1998**, *98*, 1803.

[16] R. Auzély-Velty, M. Rinaudo, *Macromolecules* **2002**, *35*, 7955.
[17] D. P. Shoemaker, C. W. Garland, J. I. Steinfeld, *Experiments in Physical Chemistry*, 2nd ed., McGraw-Hill, New York, **1974**, pp. 51–55.
[18] Cerius^2, version 3.5, Molecular Simulations, San Diego, CA, **1997**.
[19] a) J. Maple, U. Dinur, A. T. Hagler, *Proc. Natl. Acad. Sci. U.S.A.* **1988**, *85*, 5350; b) J. R. Maple, *Isr. J. Chem.* **1994**, *34*, 195; c) J. R. Maple, M. J. Hwang, T. P. Stockfisch, U. Dinur, M. Waldman, C. S. Ewing, A. T. Hagler, *J. Comput. Chem.* **1994**, *15*, 162; d) H. Sun, *Macromolecules* **1995**, *28*, 701; e) H. Sun, S. J. Mumby, J. R. Maple, A. T. Hagler, *J. Am. Chem. Soc.* **1994**, *116*, 2978.
[20] A. K. Rappe, W. A. Goddard III, *J. Phys. Chem.* **1991**, *95*, 3358.
[21] C. Betzel, W. Saenger, B. E. Hingerty, G. M. Brown, *J. Am. Chem. Soc.* **1984**, *106*, 7545.
[22] L. Verlet, *Phys. Rev.* **1967**, *159*, 98.

Received: May 25, 2007
Published online: July 26, 2007

